

Search for α and 2β decays of naturally occurring osmium nuclides accompanied by γ quanta

**V. Caracciolo^{1,2}, P. Belli^{1,2}, R. Bernabei^{1,2}, F. Cappella^{3,4}, R. Cerulli^{1,2}, F. A. Danevich^{2,5},
A. Incicchitti^{3,4}, D. V. Kasperovych⁵, V. V. Kobychiev⁵, G. P. Kovtun^{6,7,†}, N. G. Kovtun⁶,
A. Leoncini^{1,2}, M. Laubenstein⁸, V. Merlo^{1,2}, D. V. Poda⁹, O. G. Polischuk^{1,5}, A. P.
Shcherban⁶, S. Tessalina¹⁰ and V. I. Tretyak^{5,11}**

1 Dipartimento di Fisica, Università di Roma Tor Vergata, Rome, Italy

2 INFN, sezione di Roma Tor Vergata, Rome, Italy

3 INFN, sezione di Roma, Rome, Italy

4 Dipartimento di Fisica, Università di Roma 'La Sapienza', Rome, Italy

5 Institute for Nuclear Research of NASU, Kyiv, Ukraine

6 National Science Center 'Kharkiv Institute of Physics and Technology', Kharkiv, Ukraine

7 V.N. Karazin Kharkiv National University, Kharkiv, Ukraine

8 INFN, Laboratori Nazionali del Gran Sasso, Assergi (AQ), Italy

9 Université Paris-Saclay, CNRS/IN2P3, IJCLab, Orsay, France

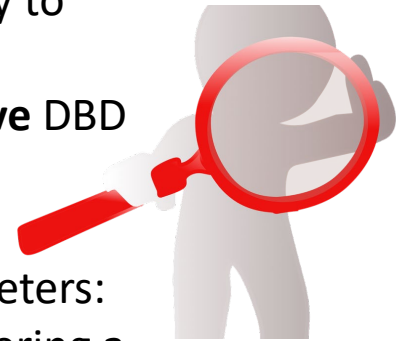
10 John de Laeter Centre for Isotope Research, Curtin University, Bentley, WA, Australia

11 Dipartimento di Fisica e Chimica, Università dell'Aquila, L'Aquila, Italy

† Deceased

INTEREST IN STUDYING THE 34 **DBD+** EMITTERS

- DBD modes without the emission of neutrinos, if observed, can open windows on **new physics**
- to **test calculations** of **different nucleus shapes** and **decay modes** that involve the vector and **axial-vector weak effective coupling constants**; possibility to study the “**resonant effect**” on the **$0\nu 2\varepsilon$ mode**;
- **mutual information** from the simultaneous study of **positive** and **negative** DBD can constrain the theoretical parameters with very high confidence
- the nuclear matrix elements for **the two-neutrino mode** and for the **neutrinoless** mode can be **related** to each other through relevant parameters: in the **free nucleon interaction, the g_A value is 1.2701**, but, when considering a nuclear decay, there are indications that the phenomenological axial-vector coupling value is reduced at **$g_A < 1$** , more precisely: **$g_A \approx 1.269 A^{-0.18}$ or $g_A \approx 1.269 A^{-0.12}$** , depending on the nuclear model adopted to infer the g_A value. DBD investigation with various nuclei would shed new light in constraining these and other important model-dependent parameters.
- search for the $0\nu EC\beta^+$ and $0\nu 2\beta^+$ decays has the potential to clarify the possible contribution of the right-handed currents to the $0\nu 2\beta^-$ decay rate
- **As byproduct**: developments of new detectors or radiopure samples, e.g., **new crystal scintillators** containing DBD emitters



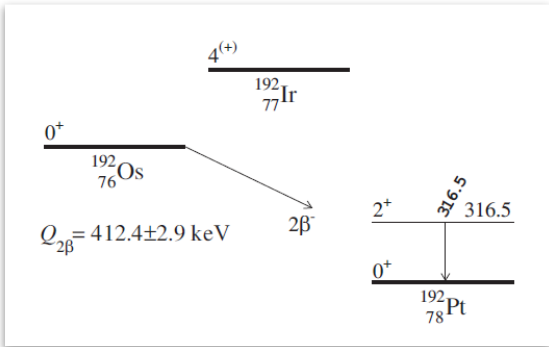
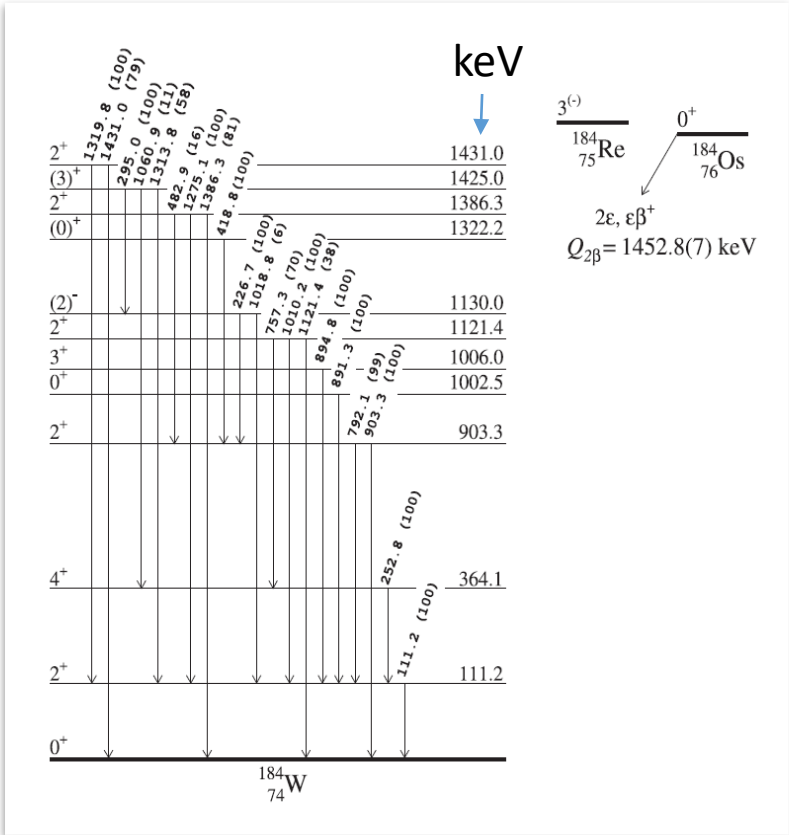
Double-beta decay of osmium

Osmium contains two potentially 2β active isotopes:

Isotope	Q [keV]	isotopic abundance [%]	Transition
^{184}Os	1452.8(7)	0.02(1)	$2\varepsilon, \varepsilon\beta^+$
^{192}Os	406(3)	40.78(32)	$2\beta^-$

(^{184}Os) Main possible processes that can be investigated by γ spectrometer technique (partial list)

Process of decay	Decay mode	Level of daughter nucleus (keV)	E_γ (keV)	
$^{184}\text{Os} \rightarrow ^{184}\text{W}$	$\varepsilon\beta^+$	g.s.	511	
	$\varepsilon\beta^+$	g.s.	511	
	$\varepsilon\beta^+$	2^+ 111.2	511	
	$\varepsilon\beta^+$	2^+ 111.2	511	
	$2K$	g.s.	58–69	
	2ε	2^+ 111.2	111.2	
	2ε	2^+ 903.3	903.3	
	2ε	0^+ 1002.5	891.3	
	2ε	2^+ 1121.4	757.3	
	$2K$	0ν	g.s.	1314.1–1315.3
	KL	0ν	g.s.	1371.5–1374.7
	$2L$	0ν	g.s.	1428.9–1433.9
	$2K$	0ν	2^+ 111.2	1202.9–1204.1
	2ε	0ν	2^+ 903.3	903.3
	2ε	0ν	0^+ 1002.5	891.3
2ε	0ν	2^+ 1121.4	757.3	



$$\Delta = Q_{2\beta} - E^* - E_{b1} - E_{b2}$$

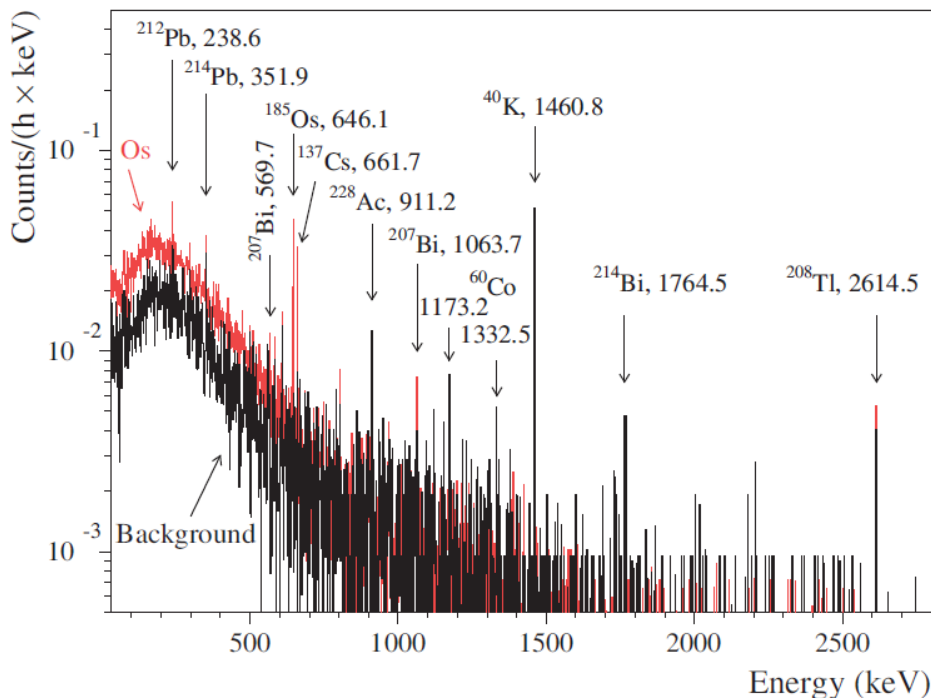
We can also consider the resonant- $0\nu 2\varepsilon$:
 $0\nu 2L: ^{184}\text{Os} \rightarrow ^{184}\text{W}, (2^+, 1431.0 \text{ keV})$

The Os sample and the first experimental set-up

[Eur. Phys. J. A \(2013\)49:24](#)

The experiment has been realized with the help of an ultra-low background **HP-Ge** detector (465 cm^3) and an ultrapure osmium sample (**173 g**, 99.999% purity) at the Gran Sasso National Laboratory of the INFN (Italy).

The detector is shielded by lead ($\approx 25 \text{ cm}$) and copper ($\approx 10 \text{ cm}$). The FWHM energy resolution of the spectrometer is 2.0 keV for the 1333 keV γ quanta of ^{60}Co



Energy spectra measured with the ultralow background HPGe γ spectrometer with the osmium sample over 2741 h (Os) and without the sample over 1046 h (Background).

The energies of the γ lines are in keV.

2β processes in ^{184}Os have been established at the level of limits on $T_{1/2} \sim 10^{14}\text{--}10^{17} \text{ y}$. Possible resonant double-electron captures in ^{184}Os were searched for with a sensitivity of $T_{1/2} \sim 10^{16} \text{ y}$.

A half-life limit $T_{1/2} \geq 5.3 \times 10^{19} \text{ y}$ (90% C.L.) was set for the 2β decay of ^{192}Os to the first excited level of ^{192}Pt .

The Os sample and the second experimental set-up

Eur. Phys. J. A (2013)49:24



The ingots were cut into thin slices with a thickness of (0.79–1.25) mm by electroerosion cutting with a brass wire in kerosene.



Journal of Physics G: Nuclear and Particle Physics 48 085104 2021

The experiment has been realized with the help of an ultra-low background broad-energy germanium detector (112.5 cm³ of active volume) and an ultrapure osmium sample (117.96(2) g) at the **Gran Sasso National Laboratory of the INFN (Italy)**.



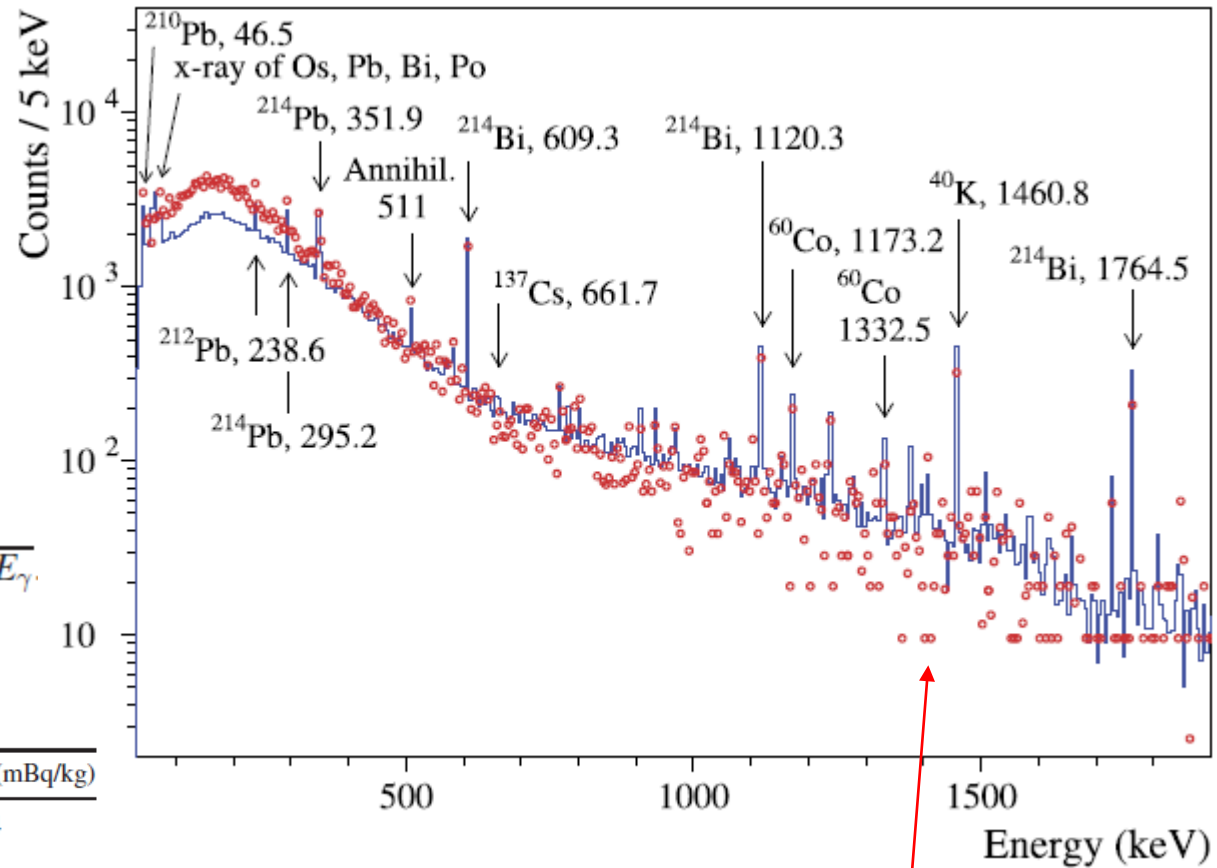
The endcap of the detector is made of 1.5 mm aluminium

The detector with the Os sample was shielded by layers of ≈ 5 cm thick high-purity copper and 20 cm thick lead.

Improved detection efficiencies and energy resolutions in the energy region from several keV to several hundreds keV.

The Os sample and the second experimental set-up

The isotopic concentration of ^{184}Os was determined as 0.0170(7)%, with an accuracy essentially higher than that of the adopted reference value of 0.02(2)%. The ^{192}Os isotopic abundance was measured as 40.86(5)% (the reference value is 40.78(32)%).



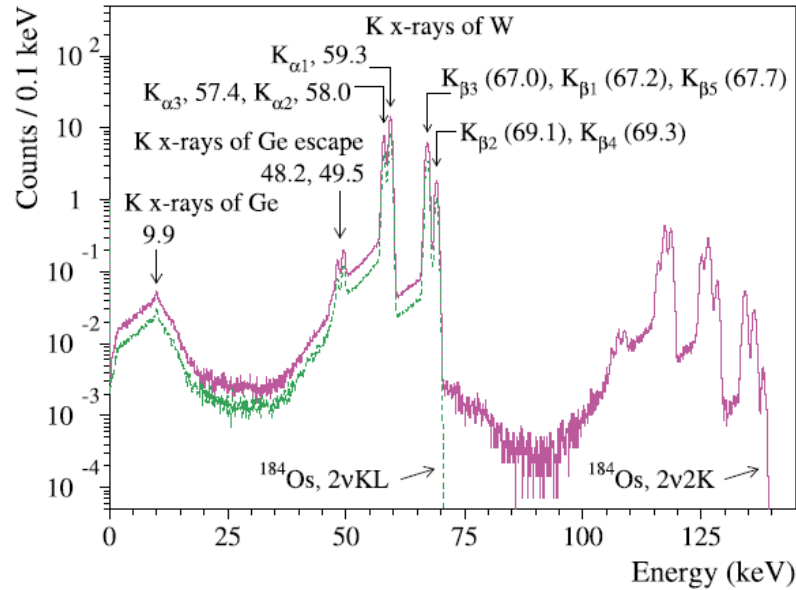
$$\text{FWHM(keV)} = 0.57(5) + 0.029(2) \times \sqrt{E_\gamma}$$

Table 1. Radioactive trace impurities in the Os sample.

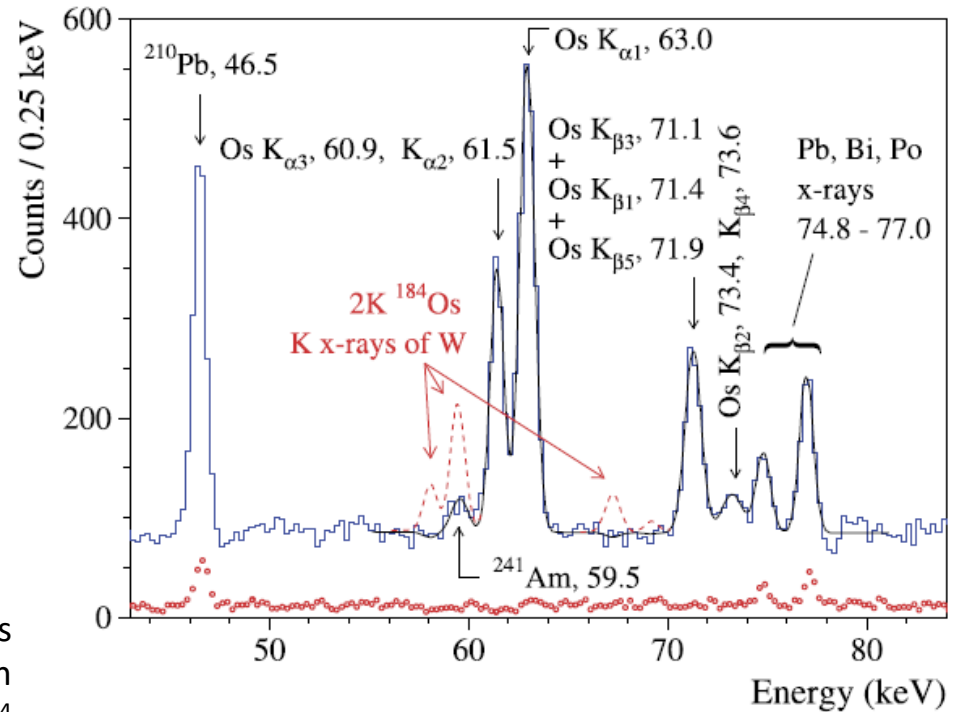
Decay chain	Radionuclide	Specific activity (mBq/kg)
	^{40}K	11 ± 4
	^{60}Co	≤ 1.3
	^{137}Cs	0.5 ± 0.1
	^{241}Am	≤ 5.6
^{232}Th	^{228}Ra	≤ 6.6
	^{228}Th	≤ 16
^{235}U	^{235}U	≤ 8.0
	^{231}Pa	≤ 3.5
	^{227}Ac	≤ 1.1
^{238}U	^{238}U	≤ 35
	^{226}Ra	≤ 4.4
	^{210}Pb	≤ 180

The Os sample and the second experimental set-up

Journal of Physics G: Nuclear and Particle Physics 48 085104 2021



Simulated energy spectra for the 2v2K and 2vKL decays of ^{184}Os assuming the experimental configuration described. Both the distributions are normalized to 10^4 decays in the Os sample.



The fastest decay of ^{184}Os is theoretically expected to be the 2v2EC, mainly absorbing the K and/or L electron shells. In case of 2v2K, 2vKL, and 2v2L capture in ^{184}Os , a cascade of x-rays and Auger electrons of the W atom is expected. However, the 2v2L decay cannot be detected in the present experiment since the energies of the L x-rays of tungsten (7.4 keV–11.7 keV) are below the detector's energy threshold

$$\lim T_{1/2} = \frac{N \cdot \ln 2 \cdot \eta \cdot t}{\lim S}$$

The Os sample and the second experimental set-up

Table 2. Half-life limits on 2β processes in ^{184}Os and ^{192}Os .

Transition	Level of daughter nucleus (keV)	E_γ (keV)	Detection efficiency	lim S	Experimental limits, $T_{1/2}$ (yr) at 90% C.L.	
					Present work	Previous result [28] (first configuration)
$^{184}\text{Os} \rightarrow ^{184}\text{W}$						
$2\nu 2K$	g.s.	57–69	2.911%	78	$\geq 3.0 \times 10^{16}$	$\geq 1.9 \times 10^{14}$
$2\nu KL$	g.s.	57–69	1.635%	65	$\geq 2.0 \times 10^{16}$	
$2\nu 2K$	$2^+ 111.2$	57–69	3.487%	78	$\geq 3.6 \times 10^{16}$	$\geq 3.1 \times 10^{15}$
$2\nu KL$	$2^+ 111.2$	57–69	1.959%	65	$\geq 2.4 \times 10^{16}$	$\geq 3.1 \times 10^{15}$
$2\nu 2EC$	$2^+ 111.2$	111.2	0.340%	37	$\geq 7.3 \times 10^{15}$	$\geq 3.1 \times 10^{15}$
$2\nu 2EC$	$2^+ 903.3$	903.3	1.230%	4.9	$\geq 2.0 \times 10^{17}$	$\geq 3.2 \times 10^{16}$
$2\nu 2EC$	$0^+ 1002.5$	891.3	2.397%	6.8	$\geq 2.8 \times 10^{17}$	$\geq 3.8 \times 10^{17}$
$2\nu 2EC$	$2^+ 1121.4$	757.3	0.802%	6.2	$\geq 1.0 \times 10^{17}$	$\geq 6.9 \times 10^{16}$
$2\nu KL$	$(0^+) 1322.2$	903.3	1.056%	4.9	$\geq 1.7 \times 10^{17}$	
$2\nu 2L$	$2^+ 1386.3$	1275.1	0.967%	26	$\geq 3.0 \times 10^{16}$	
$2\nu 2L$	$(3)^+ 1425.0$	903.3	0.518%	4.9	$\geq 8.4 \times 10^{16}$	
$2\nu 2L$	$2^+ 1431.0$	1319.8	1.002%	18	$\geq 4.4 \times 10^{16}$	
$0\nu 2K$	g.s.	1313.1–1314.5	1.838%	9.0	$\geq 1.6 \times 10^{17}$	$\geq 2.0 \times 10^{17}$
$0\nu KL$	g.s.	1370.5–1373.8	1.827%	11	$\geq 1.3 \times 10^{17}$	$\geq 1.3 \times 10^{17}$
$0\nu 2L$	g.s.	1427.9–1433.1	1.833%	20	$\geq 7.3 \times 10^{16}$	$\geq 1.4 \times 10^{17}$
$0\nu 2K$	$2^+ 111.2$	1201.9–1203.3	1.911%	20	$\geq 7.6 \times 10^{16}$	$\geq 3.3 \times 10^{17}$
$0\nu KL$	$2^+ 111.2$	57–69	1.584%	65	$\geq 1.9 \times 10^{16}$	
$0\nu 2EC$	$2^+ 903.3$	903.3	1.019%	4.9	$\geq 1.7 \times 10^{17}$	$\geq 2.8 \times 10^{16}$
$0\nu 2EC$	$0^+ 1002.5$	310.6–312.0	3.773%	14	$\geq 2.1 \times 10^{17}$	$\geq 3.5 \times 10^{17}$
$0\nu 2EC$	$2^+ 1121.4$	757.3	0.736%	6.2	$\geq 9.4 \times 10^{16}$	$\geq 6.4 \times 10^{16}$
$0\nu KL$	$(0)^+ 1322.2$	903.3	1.045%	4.9	$\geq 1.7 \times 10^{17}$	$\geq 2.8 \times 10^{16}$
$0\nu 2L$	$2^+ 1386.3$	1275.1	0.966%	26	$\geq 3.0 \times 10^{16}$	$\geq 6.7 \times 10^{16}$
$0\nu 2L$	$(3)^+ 1425.0$	903.3	0.517%	4.9	$\geq 8.4 \times 10^{16}$	

The Os sample and the second experimental set-up

Table 2. Half-life limits on 2β processes in ^{184}Os and ^{192}Os .

Transition	Level of daughter nucleus (keV)	E_γ (keV)	Detection efficiency	lim S	Experimental limits, $T_{1/2}$ (yr) at 90% C.L.	
					Present work	Previous result [28] (first configuration)
$^{184}\text{Os} \rightarrow ^{184}\text{W}$						
$2\nu 2K$	g.s.	57–69	2.911%	78	$\geq 3.0 \times 10^{16}$	$\geq 1.9 \times 10^{14}$
$2\nu KL$	g.s.	57–69	1.635%	65	$\geq 2.0 \times 10^{16}$	
$2\nu 2K$	$2^+ 111.2$	57–69	3.487%	78	$\geq 3.6 \times 10^{16}$	$\geq 3.1 \times 10^{15}$
$2\nu KL$	$2^+ 111.2$	57–69	1.959%	65	$\geq 2.4 \times 10^{16}$	$\geq 3.1 \times 10^{15}$
$2\nu 2EC$	$2^+ 111.2$	111.2	0.340%	37	$\geq 7.3 \times 10^{15}$	$\geq 3.1 \times 10^{15}$
$2\nu 2EC$	$2^+ 903.3$	903.3	1.230%	4.9	$\geq 2.0 \times 10^{17}$	$\geq 3.2 \times 10^{16}$
$2\nu 2EC$	$0^+ 1002.5$	891.3	2.397%	6.8	$\geq 2.8 \times 10^{17}$	$\geq 3.8 \times 10^{17}$
$2\nu 2EC$	$2^+ 1121.4$	757.3	0.802%	6.2	$\geq 1.0 \times 10^{17}$	$\geq 6.9 \times 10^{16}$
$2\nu KL$	$(0^+) 1322.2$	903.3	1.056%	4.9	$\geq 1.7 \times 10^{17}$	
$2\nu 2L$	$2^+ 1386.3$	1275.1	0.967%	26	$\geq 3.0 \times 10^{16}$	
$2\nu 2L$	$(3)^+ 1425.0$	903.3	0.518%	4.9	$\geq 8.4 \times 10^{16}$	
$2\nu 2L$	$2^+ 1431.0$	1319.8	1.002%	18	$\geq 4.4 \times 10^{16}$	
$0\nu 2K$	g.s.	1313.1–1314.5	1.838%	9.0	$\geq 1.6 \times 10^{17}$	$\geq 2.0 \times 10^{17}$
$0\nu KL$	g.s.	1370.5–1373.8	1.827%	11	$\geq 1.3 \times 10^{17}$	$\geq 1.3 \times 10^{17}$
$0\nu 2L$	g.s.	1427.9–1433.1	1.833%	20	$\geq 7.3 \times 10^{16}$	$\geq 1.4 \times 10^{17}$
$0\nu 2K$	$2^+ 111.2$	1201.9–1203.3	1.911%	20	$\geq 7.6 \times 10^{16}$	$\geq 3.3 \times 10^{17}$
$0\nu KL$	$2^+ 111.2$	57–69	1.584%	65	$\geq 1.0 \times 10^{16}$	

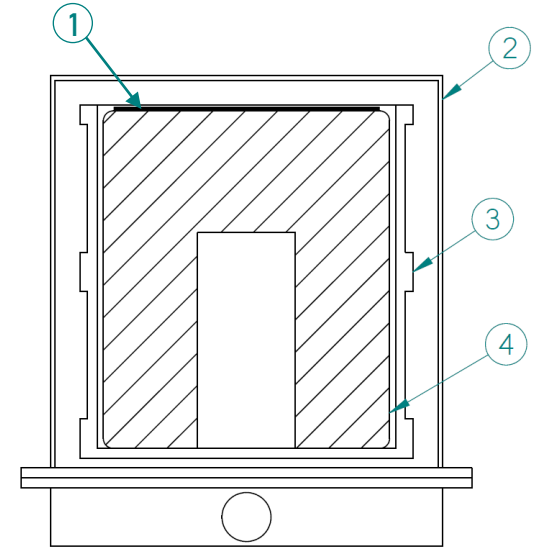
Table 2. Continue

Resonant $0\nu 2L$	$2^+ 1431.0$	1319.8	1.005%	18	$\geq 4.4 \times 10^{16}$	$\geq 8.2 \times 10^{16}$
$2\nu EC\beta^+$	g.s.	511	7.526%	58	$\geq 1.0 \times 10^{17}$	$\geq 2.5 \times 10^{16}$
$2\nu EC\beta^+$	$2^+ 111.2$	511	7.271%	58	$\geq 1.0 \times 10^{17}$	$\geq 2.5 \times 10^{16}$
$0\nu EC\beta^+$	g.s.	511	7.403%	58	$\geq 1.0 \times 10^{17}$	$\geq 2.5 \times 10^{16}$
$0\nu EC\beta^+$	$2^+ 111.2$	511	7.191%	58	$\geq 9.9 \times 10^{16}$	$\geq 2.4 \times 10^{16}$
$^{192}\text{Os} \rightarrow ^{192}\text{Pt}$						
$2\beta^- (2\nu + 0\nu)$	$2^+ 316.5$	316.5	4.820%	45	$\geq 2.0 \times 10^{20}$	$\geq 5.3 \times 10^{19}$

Present configuration of the experiment with Os

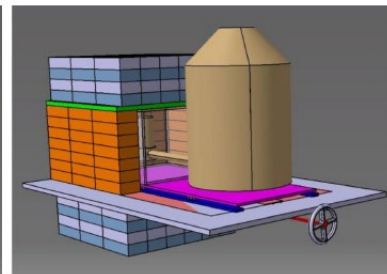
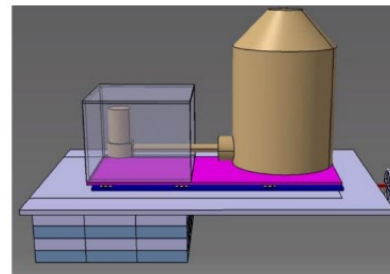


The main part of the osmium slices before assembling on a plastic support plate placed directly in the HP-Ge cryostat

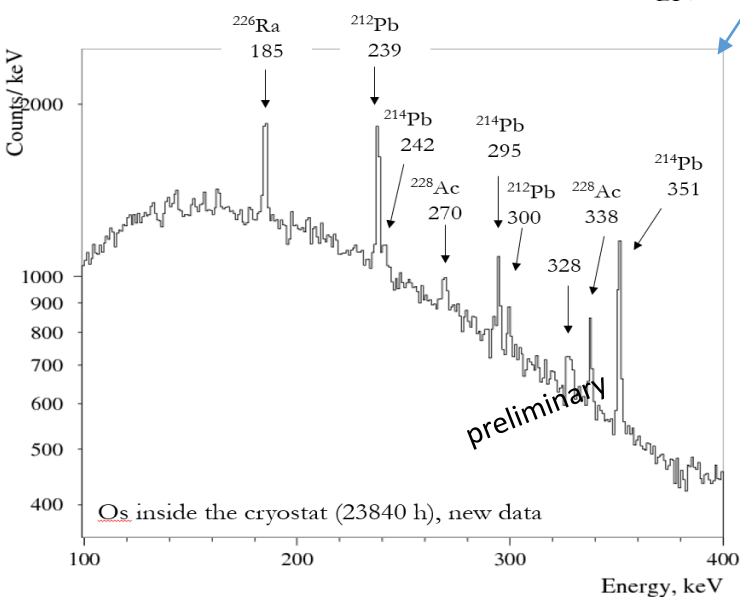
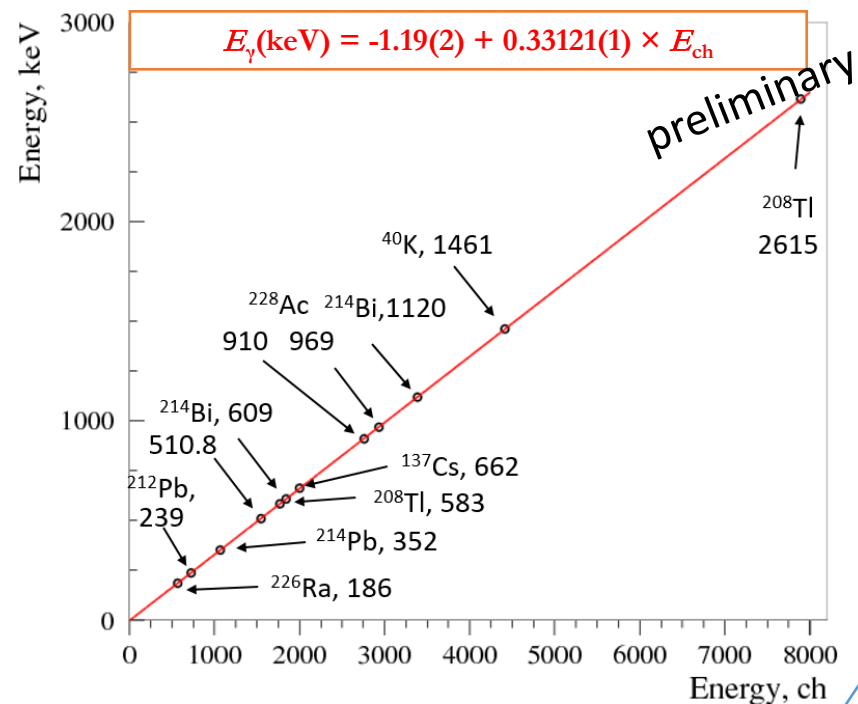


1) sample; 2) detector end cap; 3) crystal holder; 4) Ge crystal

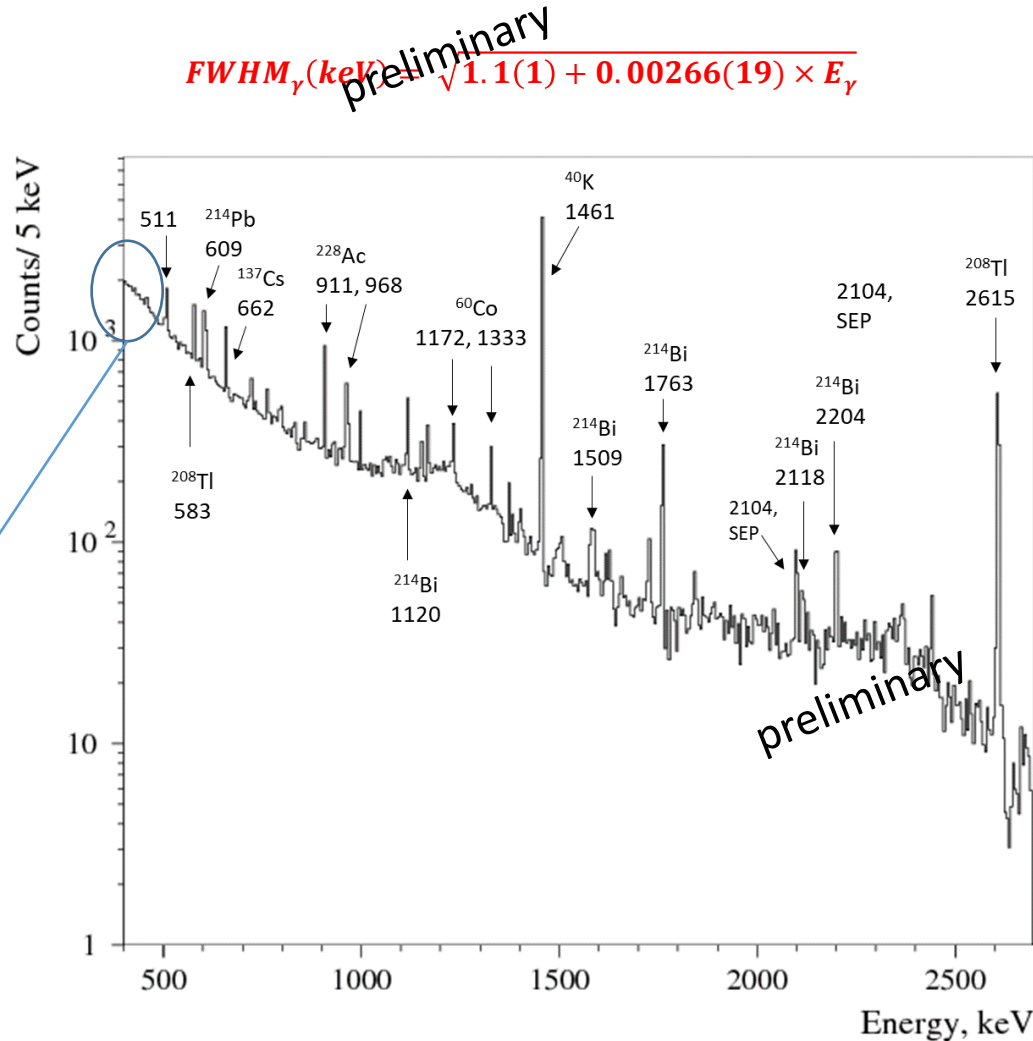
Osmium metal pieces (**58.78 g**) glued to the plastic plate have been placed inside the HP-Ge detector cryostat directly on the Ge crystal (**250 cm³ of active volume**) at LNGS.



Present configuration: first look at the collected data

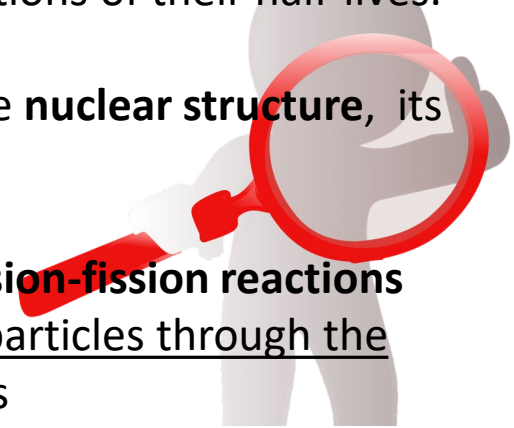


Os inside the cryostat (23840 h), new data



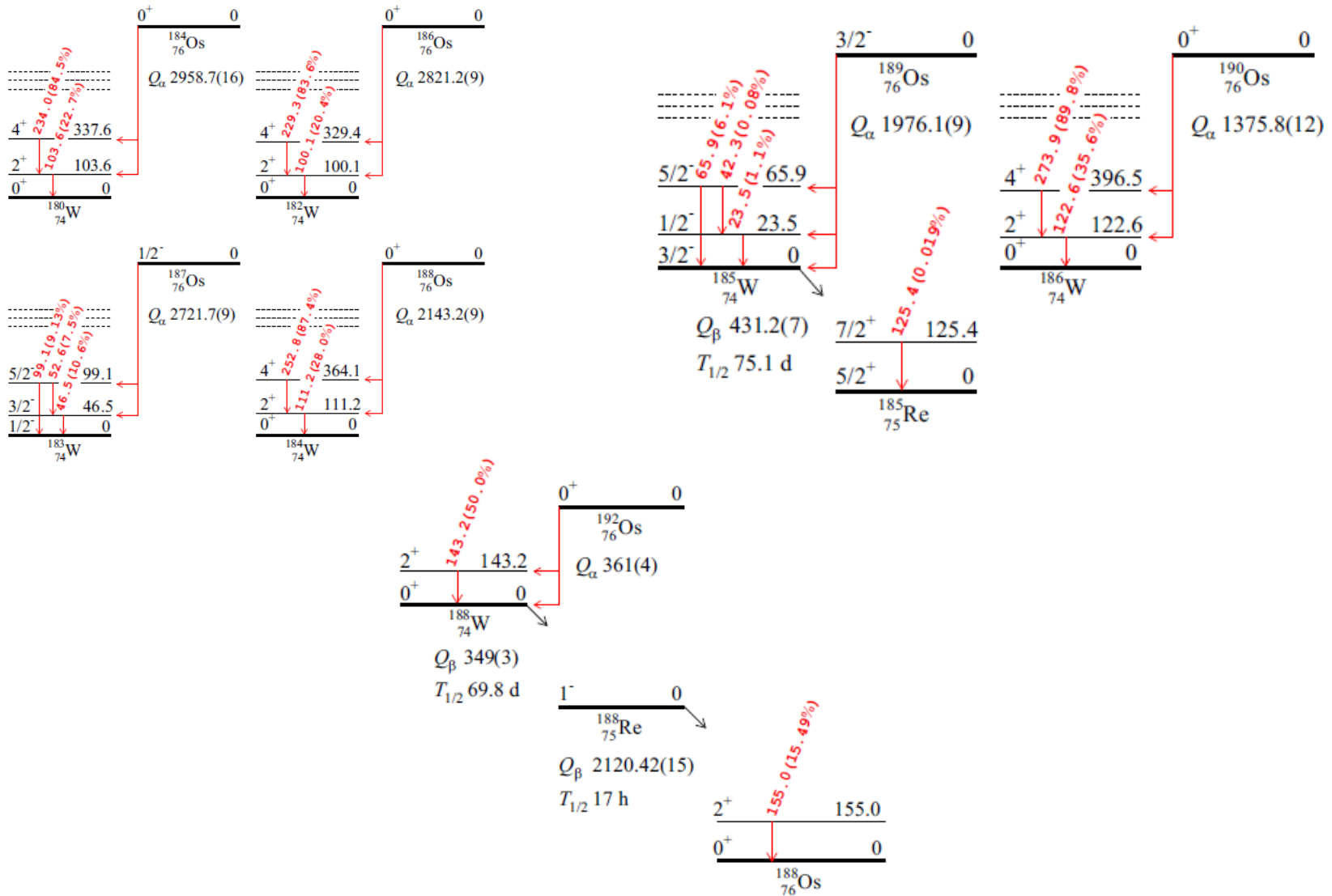
INTEREST IN STUDYING RARE α DECAY

- Various **theoretical models are continuously developed or improved**, e.g., motivated by searches for stable or long-lived superheavy isotopes and predictions of their half-lives.
- The study on the **nuclear instability offers information** about the **nuclear structure, its levels** and the properties of nuclei.
- The phenomenon of α decay can offer information about the **fusion-fission reactions** since the α decay process involves sub-barrier penetration of α particles through the barrier, caused by the interaction between the α and the nucleus
- Understanding the nuclear properties is essential also for nuclear and particle astrophysics studies, for example, **α -capture reactions** (equivalent to the inverse α -decay process) are important for the **nucleosynthesis** and the **β -delayed fission**, together with other fission modes, determine the so-called “**fission recycling**” in the **r-process** nucleosynthesis.
- Among the naturally occurring α -emitting nuclides only those with either $A > 208$ or $A \approx 145$ have α half-lives short enough to be detected
- **As byproduct**: developments of new detectors or radiopure samples, e.g., new crystal scintillators containing α emitters



Rare alpha decay of Osmium

Some possible processes that can be investigated by γ spectrometer technique



Rare alpha decay of Osmium (second experimental stage)

PHYSICAL REVIEW C 102, 024605 (2020)

Transition, J^π , E (keV)	Q_α (keV)	Partial $T_{1/2}$ (yr)				Experimental
		Theoretical				
	[22]	[23]	[24,25]	[5]	[11]	
$^{184}\text{Os}, 0^+ \rightarrow ^{180}\text{W}, 0^+, \text{g.s.}$	2958.7(16)	7.2×10^{13}	3.5×10^{13}	3.3×10^{13}	2.1×10^{13}	$> 2.0 \times 10^{13}$ [17] $> 5.6 \times 10^{13}$ [19] $= (1.1 \pm 0.2) \times 10^{13}$ [20]
$^{184}\text{Os}, 0^+ \rightarrow ^{180}\text{W}, 2^+, 103.6$		2.9×10^{15}	1.3×10^{15}	6.3×10^{14}	7.3×10^{14}	$\geq 6.8 \times 10^{15}$ this work
$^{184}\text{Os}, 0^+ \rightarrow ^{180}\text{W}, 4^+, 337.6$		2.5×10^{19}	1.0×10^{19}	9.2×10^{17}	4.6×10^{18}	$\geq 4.6 \times 10^{16}$ this work
$^{186}\text{Os}, 0^+ \rightarrow ^{182}\text{W}, 0^+, \text{g.s.}$	2821.2(9)	4.7×10^{15}	1.9×10^{15}	1.6×10^{15}	1.0×10^{15}	$= (2.0 \pm 1.1) \times 10^{15}$ [21]
$^{186}\text{Os}, 0^+ \rightarrow ^{182}\text{W}, 2^+, 100.1$		2.2×10^{17}	8.3×10^{16}	3.3×10^{16}	3.9×10^{16}	$\geq 3.3 \times 10^{17}$ this work
$^{186}\text{Os}, 0^+ \rightarrow ^{182}\text{W}, 4^+, 329.4$		2.9×10^{21}	9.7×10^{20}	7.2×10^{19}	3.7×10^{20}	$\geq 6.0 \times 10^{18}$ this work
$^{187}\text{Os}, 1/2^- \rightarrow ^{183}\text{W}, 1/2^-, \text{g.s.}$	2721.7(9)	4.5×10^{19}	4.1×10^{16}	5.1×10^{16}	2.0×10^{16}	–
$^{187}\text{Os}, 1/2^- \rightarrow ^{183}\text{W}, 3/2^-, 46.5$		4.4×10^{20}	3.6×10^{17}	6.7×10^{18}	1.6×10^{17}	$\geq 3.2 \times 10^{15}$ this work
$^{187}\text{Os}, 1/2^- \rightarrow ^{183}\text{W}, 5/2^-, 99.1$		2.8×10^{21}	2.1×10^{18}	4.0×10^{19}	9.1×10^{17}	$\geq 1.9 \times 10^{17}$ this work
$^{188}\text{Os}, 0^+ \rightarrow ^{184}\text{W}, 0^+, \text{g.s.}$	2143.2(9)	6.8×10^{26}	1.4×10^{26}	7.2×10^{25}	5.2×10^{25}	–
$^{188}\text{Os}, 0^+ \rightarrow ^{184}\text{W}, 2^+, 111.2$		2.9×10^{29}	5.5×10^{28}	1.3×10^{28}		$\geq 3.3 \times 10^{18}$ this work
$^{188}\text{Os}, 0^+ \rightarrow ^{184}\text{W}, 4^+, 364.1$		1.9×10^{36}	2.7×10^{35}	8.9×10^{33}		$\geq 5.0 \times 10^{19}$ this work
$^{189}\text{Os}, 3/2^- \rightarrow ^{185}\text{W}, 3/2^-, \text{g.s.}$	1976.1(9)	2.4×10^{34}	4.8×10^{29}	3.1×10^{29}		$\geq 3.5 \times 10^{15}$ this work
$^{189}\text{Os}, 3/2^- \rightarrow ^{185}\text{W}, 1/2^-, 23.5$		1.8×10^{35}	3.2×10^{30}	1.1×10^{32}		$\geq 3.5 \times 10^{15}$ this work
$^{189}\text{Os}, 3/2^- \rightarrow ^{185}\text{W}, 5/2^-, 65.9$		2.1×10^{36}	3.1×10^{31}	1.1×10^{33}		$\geq 7.6 \times 10^{17}$ this work
$^{190}\text{Os}, 0^+ \rightarrow ^{186}\text{W}, 0^+, \text{g.s.}$	1375.8(12)	3.6×10^{48}	2.0×10^{47}	2.1×10^{46}		–
$^{190}\text{Os}, 0^+ \rightarrow ^{186}\text{W}, 2^+, 122.6$		1.1×10^{54}	4.9×10^{52}	1.6×10^{51}		$\geq 1.2 \times 10^{19}$ this work
$^{190}\text{Os}, 0^+ \rightarrow ^{186}\text{W}, 4^+, 396.5$		5.8×10^{69}	1.1×10^{68}	1.6×10^{65}		$\geq 8.6 \times 10^{19}$ this work
$^{192}\text{Os}, 0^+ \rightarrow ^{188}\text{W}, 0^+, \text{g.s.}$	361(4)	1.7×10^{153}	1.8×10^{149}	1.4×10^{140}		$\geq 5.8 \times 10^{18}$ this work
$^{192}\text{Os}, 0^+ \rightarrow ^{188}\text{W}, 2^+, 143.2$		1.6×10^{215}	5.5×10^{209}	9.9×10^{190}		$\geq 2.7 \times 10^{19}$ this work

Conclusions

2 β decays

Using a ultra-pure osmium samples installed on the endcap of a ultra-lowbackground broad-energy germanium detectors, new limits on double-electron capture and electron capture with positron emission in ^{184}Os were set at the level of $T_{1/2} > 10^{16}\text{--}10^{17}$ yr.

In particular the **2 ν 2K** and **2 ν KL** decays of ^{184}Os to the **g.s. of ^{184}W** are restricted as $T_{1/2} > 3.0 \times 10^{16}$ yr and $T_{1/2} > 2.0 \times 10^{16}$ yr, respectively.

A lower limit on the half-life for the double-beta decay of ^{192}Os to the **first excited level of ^{192}Pt** was set as $T^{1/2} > 2.0 \times 10^{20}$ yr at 90% C.L.

α decays

Lower limits on the processes were set at level of $T_{1/2} > 10^{15}\text{--}10^{19}$ yr.

The half-life limits for **α decays of ^{184}Os** and ^{186}Os to the first excited levels of daughter nuclei have been set at 90% C.L. as $T_{1/2} > 6.8 \times 10^{15}$ yr and $T_{1/2} > 3.3 \times 10^{17}$ yr, respectively. The limits **exceed substantially** the present **theoretical estimations** of the decays probabilities that are within $T_{1/2} \approx (0.6\text{--}3) \times 10^{15}$ yr for ^{184}Os and $T_{1/2} \approx (0.3\text{--}2) \times 10^{17}$ yr for ^{186}Os .

2 β and α decays

A **new stage** of the experiment is in progress by using an advanced geometry with the osmium sample placed **directly** on the HP-Ge detector **inside its cryostat** to **increase** the **detection** efficiency to the **low-energy γ -ray quanta** expected in the theoretically fastest decays of ^{184}Os and ^{186}Os to the first excited levels of the daughter nuclei.

Osmium isotopes could be enriched by gas centrifugation, at present the only viable technology to produce large amounts of isotopically enriched materials. Using of enriched isotopes can improve dramatically the sensitivity of experiments with ^{184}Os and ^{186}Os . In particular the alpha decays of these nuclides to excited levels of the daughters can be surely observed.